PhD Thesis

Analysis of water vapor diffusion in structural wood adhesive bond

By

Omar Saber Zinad

Supervisor:

Mrs. Dr. habil. Csilla CSIHA

University of Sopron

Faculty of Wood Engineering and Creative Industries

Cziráki József Doctoral School of Wood Sciences and Technologies

Head: Prof. Dr. László Bejó

Sopron, 2026

Abstract

Wood-based construction materials have become a new alternative to modern sustainable engineering due to their favorable environmental impact, excellent mechanical properties, and suitability for replacing energy-intensive building materials such as concrete and steel. However, the hygroscopic nature of wood and its sensitivity to water-vapor exchange remain major challenges that influence mechanical performance, dimensional stability, and long-term durability. In complex wood assemblies especially in layered and adhesive-bonded systems such as cross-laminated timber (CLT) moisture transport becomes more complicated, as adhesives may block or restrict diffusion pathways, producing large internal moisture gradients that generate internal strains. Although moisture diffusion in solid wood has been widely studied, significant knowledge gaps remain regarding vapor transport in layer-bonded wood products and adhesive interfaces, the blocking-induced strains that develop at bond lines, and the feasibility of designing adhesives that permit controlled vapor transmission to reduce these strains and extend structural service performance. This thesis addresses these gaps by systematically evaluating water-vapor permeability through seven distinct wood species beech (BW), oak (OW), spruce (SW), grey poplar (GPW), smaragdfa(SMW), eucalyptus (EUW), and oil-palm wood (OPW) in uncoated, lasure-coated, adhesive-coated, and custom-made polymer–coated samples. The work investigates permeability behavior in both the pre-steady and the steady-state zones, examines the influence of adhesive molecular weight (MW), and quantifies the resulting internal strains during accelerated vapor exposure. The study further develops empirical models describing permeability-time behavior and demonstrates how the adhesive MW can be tuned to match the vapor permeability of each wood species, offering new guidelines for optimizing adhesive formulations used in structural wooden assemblies.

Water-vapor permeability tests were performed using an accelerated cup method based on ISO 12572 and ASTM E96, employing a specially designed steam chamber operating at 100% RH and ~100 °C to intensify vapor transport while preserving the relative permeability behavior among samples. Each wood disk (100 mm diameter, 10 mm thickness) was conditioned to 12% MC and mounted on an aluminum cup sealed with silicone. Uncoated specimens and specimens coated with lasure, commercial structural adhesive (A_J), experimental adhesive (A_X), and five custom-made synthesized polymers (S_1–S_5 with MW ranging from 2000 to 6000 Da) were tested. A total of 315 samples were evaluated, each weighed periodically for over 15 days. Using Statistica V2025, the permeability curve of each sample was modeled to identify the transition point (A), separating the non-linear pre-steady zone from the linear steady-state zone a distinction often overlooked in permeability studies but evidentiated here to be essential.

Diffusion behavior of uncoated wood

The steady-state permeability coefficients (δ) of uncoated specimens showed remarkably narrow variation among the seven wood species, ranging between 2.62–3.81 $\times 10^{-14}$ kg/(m·s·Pa), despite their large density differences. However, the pre-steady permeability coefficients exhibited wide variation from 44.46 $\times 10^{-14}$ in dense BW (760 kg/m³) to 82.94 $\times 10^{-14}$ in OPW (300 kg/m³). Even though δ values appeared similar in the steady state, the mass change at the transition point revealed dramatic differences: ~18.5 g (OPW), ~11 g (GPW), and only ~7.8–9 g for denser species like BW and EUW. These findings confirm that the steady-state zone masks critical permeability phenomena, whereas the pre-steady zone exposes the influence of wood anatomy porosity, vessel structure, and density on vapor uptake and transport.

Lasure-coated samples

Lasure coatings exhibited a semi-permeable behavior aligned with their formulation principles. Across species, steady-state δ ranged between 1.34–6.12

$\times 10^{-14}$, while pre-steady δ ranged between 15.71–41.94 $\times 10^{-14}$. Low-density species (OPW, SMW) reached the highest permeability values and mass change due to large accessible voids, whereas dense woods (EUW, BW) maintained limited mass gain. Lasure-treated samples exhibited stable permeability curves and moderate strain response, confirming that lasures support vapor transmission while reducing liquid-water sorption a critical property for outdoor coatings.

Adhesive-coated samples

The commercial structural adhesive (AJ) showed powerful vapor-blocking behavior. Steady-state δ values were extremely low (0.08–0.36 $\times 10^{-14}$), and mass change strongly reflected wood density: OPW (~1.34 g), SMW (~1.05 g), while dense EUW showed the lowest (~0.60 g). The …..(AX) provided slightly higher vapor permeability for several species, indicating that adhesive chemistry affects permeability beyond the influence of density alone. Spruce coated with AJ (SWAJ) had δ = 0.08 $\times 10^{-14}$ and mass change = 0.37 g, whereas SW_{AX} showed δ = 0.24 $\times 10^{-14}$ and mass change = 0.77 g. These differences highlight how polymer structure governs blocking efficiency.

Permeability with custom-made synthesized polymers (S1–S5)

Polymer systems with MW ranging from 2000–6000 Da produced systematic, density-dependent permeability behavior. In both pre-steady and steady-state zones, permeability followed the anatomical hierarchy of the wood species: OPW > SMW > GPW > SW > OW > BW > EUW. Low-MW systems (S1) exhibited more restrictive permeability while high-MW systems (S5) allowed the highest vapor transfer, occasionally enabling partial passage of water molecules. Yet, density still strongly modulated the mass change. Notably, permeability coefficients among different MW systems within the same species remained relatively close, while mass changes diverged significantly demonstrating that mass change is highly density-dependent, even when δ is similar.

Internal-strain behavior

Internal strains induced by water-vapor permeability were measured for selected specimens of BW, SW, and GPW using strain gauges under accelerated exposure to vapor from boiling water. Uncoated GPW reached the highest strains (~1650–1700 μm/m), SW stabilized around ~550 μm/m, while BW remained the least affected (~140 μm/m). Lasure produced smooth, stable strain curves (GPW ~1150–1200 μm/m; SW ~950–1000 μm/m; BW ~150–180 μm/m), reflecting controlled vapor permeability. Adhesive AJ generated the strongest strain responses (~1500–1600 μm/m for GPW; ~1100–1200 μm/m for SW; shifting toward –1100 μm/m for BW), demonstrating its blocking nature and tendency toward crack-induced relaxation in porous species. Series 5 adhesive exhibited smoother curves, moderate permeability, and reduced strain amplitudes (~650–700 μm/m in GPW; ~400–500 μm/m in SW; ~–300 ± 50 μm/m in BW). These results indicate a direct relationship between permeability resistance and internal strain: strong barriers produce large strain gradients, whereas semi-permeable systems relieve strain.

Modeling and interpretation

Mass change over time for all samples wood combinations was successfully fitted by the generalized tangential function:

$$\Delta m = b_1 * \tanh(b_0 * t) \qquad [\boldsymbol{g}]$$

where b_0 and b_1 are species- and MW-specific. This model reflects the physical behavior of permeability-driven uptake, rapid initial transport, and eventual stabilization into the steady state.

The research pillars

This thesis explores the relationship between water vapor diffusion through the adhesive layer, by:

1.) Evaluating the diffusion mechanisms in accelerated conditions on seven wood species with and without an adhesive layer, in similar conditions to

examine the diffusion properties when vapor movement is perpendicular to the bond line, in order to find that adhesive, which has the most appropriate diffusion characteristic to lasure coated wood.

2.) Adjusting the diffusion properties of adhesive materials:

one commercial structural adhesive frequently used also in CLT manufacturing and one custom-made adhesive manufactured by BorsodChem company were evaluated for their water vapor diffusion characteristics, compared with five custom-made adhesives specially designed to these experiments, formulated with different molecular weight (MW) by BorsodChem, to monitor how different polymer structures influence diffusion rates and how blocked voids within the adhesive layers contribute to strain development.

3.) Investigation of the strains:

Internal strain measurements in the adhesive layer were performed to investigate the water vapor diffusion–blocking effect of the commercial adhesives. Similar measurements with custom-made adhesives were also performed to evidentiate the difference.

4.) Comparative evaluation of the results:

By analyzing water vapor diffusion and strain development across multiple wood species with and without adhesive layer, the research can identify wood species, -and MW specific behaviors and their implications for adhesive formulation/manufacturing and selection.

5.) Identification of knowledge gaps and future research directions:

results are provided on different MW adhesive formulations, water vapor diffusion mechanisms on structurally bonded wood assemblies, within the circumstances of accelerated diffusion testing. Further research might be needed to follow the real case scenario.

This thesis aims to highlight that contrary to the actual practice structural adhesives should be formulated by the producer considering their water vapor diffusion performance. It is suggested that water vapor diffusion should be aligned with the diffusion characteristics of the lasures, which are formulated for decades upon these principles.

Material and method

Wood materials. Seven defect-free wood species were used: beech (BW), oak (OW), spruce (SW), grey poplar (GPW), Smaragdfa® paulownia hybrid (SMW), eucalyptus (EUW), and oil palm wood (OPW). Boards were taken from healthy trunks, cleaned, cut to preserve anatomical orientation, and conditioned to ~12% moisture content before specimen preparation. A total of 315 specimens were prepared (7 species × 9 surface conditions × 5 replicates).

Surface conditions and coating materials**.** Each species was tested in nine conditions: uncoated, lasure-coated, two commercial structural adhesives (AJ and AX), and five custom-synthesized resin systems (S1–S5; varied polyol molecular weight). The lasure was a commercial door/window lasure (OBI product). The commercial adhesive AJ was Jowat SE **Jowapur® 681.60** (1K PUR structural adhesive). The AX adhesive (XP 1166) and the S1–S5 resin series were provided by BorsodChem.

Specimen preparation**.** Boards were dried/conditioned, sanded to a uniform thickness, and coatings were applied on one face using controlled application (target ~150 g/m²) in thin layers to minimize foaming and ensure a continuous film. After drying (~24 h), disk specimens (Ø ~100 mm; thickness 10 mm) were cut using a crown drill, and edges were sealed to aluminum cups using a silicone sealant to ensure vapor-tight assembly. Conditioning and preparation followed ISO small-clear wood specimen practices where applicable.

Water-vapor diffusion test (cup method). Water-vapor transmission was measured using an accelerated cup method consistent with ISO ISO 12572:2016 and ASTM International ASTM E96/E96M principles. Aluminum cups were filled with silica gel (RH≈0% inside the cup). Specimens were exposed to high-humidity conditions (RH≈100%) in a sealed warm-mist chamber, and mass was recorded repeatedly over ~15.6 days (≥20 measurements per specimen). Water-vapor flow rate **G** was obtained from the slope of mass change vs. time in the linear region, and permeability **δ** was calculated from standard cup-method equations using specimen thickness, exposed area, and vapor-pressure difference.

Identification of pre-steady/steady regions. For each specimen, the transition point A (between non-linear pre-steady and linear steady behavior) was determined by regression-based curve fitting, and steady-state parameters were computed from the linear region. Curve modeling and extraction of point A were performed using Statistica (v2025).

Influence of wood density and adhesive molecular weight on water vapor diffusion

Water vapor diffusion was comprehensively assessed across all investigated wood species by comparing each coated configuration with its corresponding untreated reference sample, thereby enabling a quantitative evaluation of the vapor-blocking efficiency imparted by the different coating adhesive systems. Fig 1 and 2 illustrate the ratios of water vapor permeability δ_n of uncoated specimens to the corresponding permeabilities of coated systems δS1–δS5, δAJ, δAX, and δL for BW, OW, SW, GPW, SMW, EUW, and OPW. These comparative ratios are presented for both the steady-state and pre-steady zones, enabling a comprehensive assessment of how each adhesive formulation modifies vapor transport behavior under stabilized and early-stage diffusion conditions.

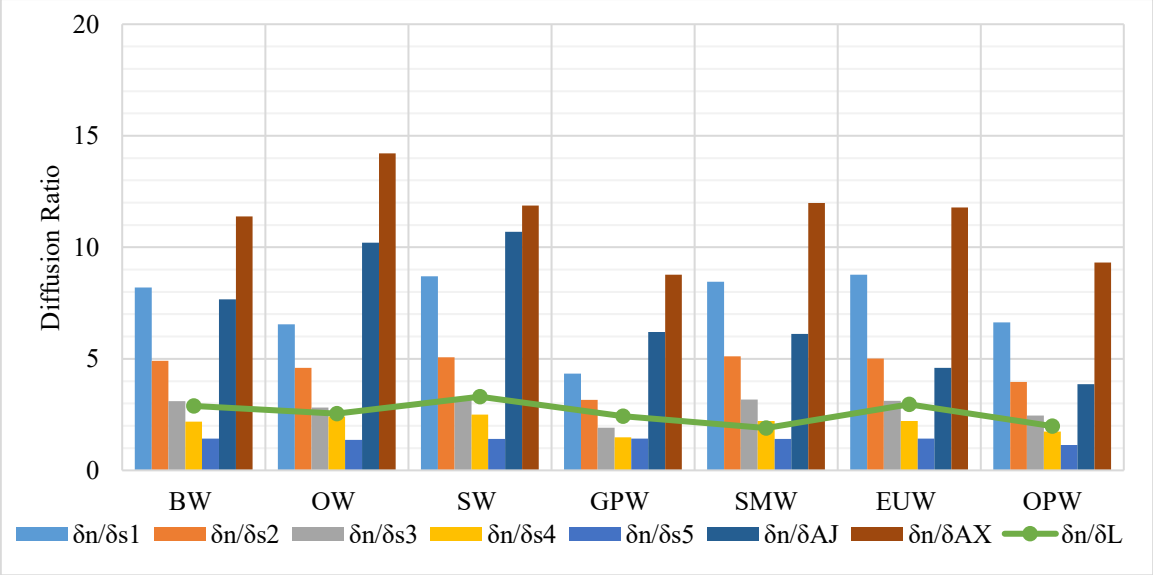

Figure 1 Water vapor permeability ratios of uncoated and differently coated wood materials in the pre--steady zone

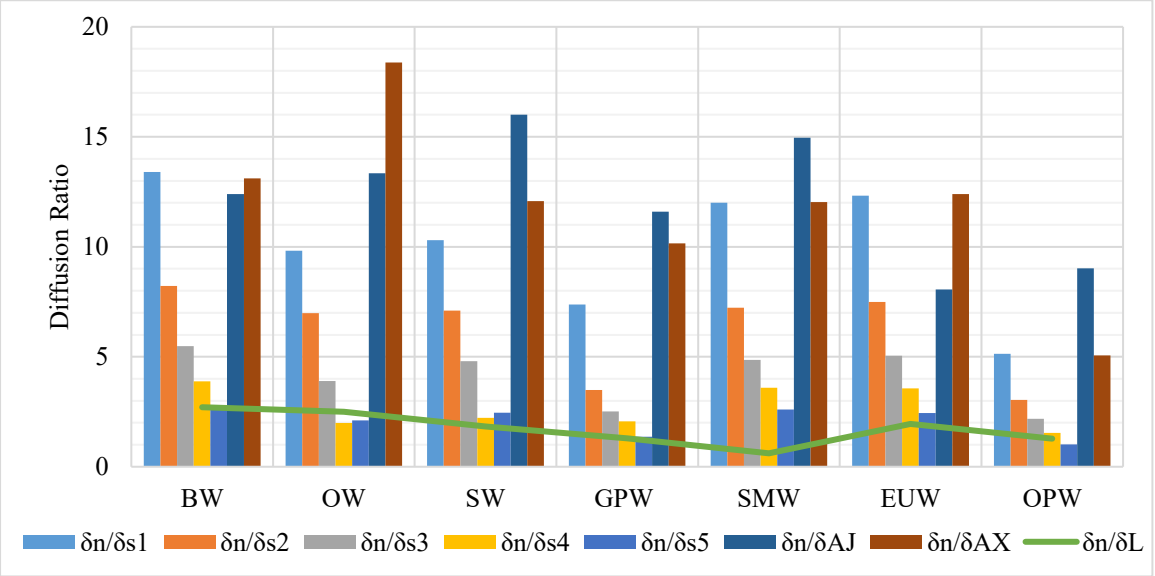

Figure 2 Water vapor permeability ratios of uncoated and differently coated wood materials in the steady zone

1- Uncoated wood

As shown in Fig. 1 and 2, the water vapor permeability values obtained in the pre-steady state exhibit a substantially wider variation between wood species compared with those measured under steady-state conditions. Whereas the steady-state permeabilities of uncoated wood species fall within a relatively narrow and comparable range between 2.62×10^{-14} kg/(m·s·Pa) and 3.81×10^{-14}

kg/(m·s·Pa), the pre-steady permeability coefficients show pronounced differences, extending from 44.46 × 10^{-12} kg/(m²·s·Pa) to 82.94 × 10^{-12} kg/(m²·s·Pa). This wider spread is directly linked to wood density: low-density species like OPW and SMW, with 301.1 kg/m^3 and 379.4 kg/m^3 respectively, exhibited the highest pre-steady-state permeability values, whereas high-density species like BW with 759.9 kg/m^3 and EUW with 952.18 kg/m^3, showed lower steady-state permeability. By doing Pearsons correlation, resulted: $r = -0.933$, $R^2 = 0.871$, $p = 0.002$, a strong and statistically significant negative correlation between wood density and **pre-steady-state** permeability, confirming that lower-density species exhibit substantially higher initial permeability coefficients. While EUW displays a modest departure from the fitted regression line, the overall trend remains robust and statistically significant. The mass change, represented by the y-coordinate of the transition point "A", follows the same trend, further confirming that the pre-steady zone reflects the rapid initial response of the material to water vapor exposure. This phase provides an early and sensitive indication of diffusion behavior, clearly demonstrating the influence of wood density on mass uptake in uncoated wood species.

Unlike pre-steady-state permeability, no significant Pearsons correlation was observed between wood density and **steady-state permeability** ($r = -0.114$, $R^2 = 0.013$, $p = 0.808$), indicating that steady-state vapor transport is essentially independent of density. The correlation is **very weak and negative. Only ~1.3% of the variability in steady-state permeability is explained by density. The relationship is not statistically significant, meaning steady-state permeability is largely independent of wood density.**

When both diffusion zones are evaluated together, it becomes evident that although different wood species exhibit similar behavior under steady-state conditions, the pre-steady region reveals the actual impact of density and anatomical structure on early-stage vapor transport. Consequently, the pre-

steady analysis delivers critical insight into diffusion mechanisms that cannot be fully captured by steady-state permeability values alone.

Based on diffusion tests performed on uncoated wood samples from seven wood species, the conclusion was deduced, that **density strongly affects pre-steady diffusion, but not the steady-state permeability behaviour**.

Table 1 permeability/mass change within uncoated wood samples

	Density Kg/m^3	δ (steady state) $\times10^{-14}$ kg/(m·s·Pa)	δ (pre-steady zone) $\times10^{-14}$ kg/(m·s·Pa)	Mass change at transition point (g)
OPW	301.1	2.68	82.94	18.5
SMW	379.4	3.72	70.24	11.36
GPW	449.3	3.68	66.10	10.99
SW	511.4	2.93	60.70	9.32
OW	682.1	3.44	55.02	9.74
BW	759.9	3.81	44.46	9.27
EUW	952.18	2.62	46.40	7.77

2- Wood coated with lasure

The wood samples coated with lasure exhibited semi-permeable behavior across all investigated wood species, as illustrated in Fig. 1 and 2. In each case, the vapor permeability of the lasure-coated specimens remained proportionally related to that of the corresponding uncoated reference, indicating moderated but not fully restricted water vapor diffusion. The wide variation in wood density (301.1–952.18 kg/m³) makes the steady-state water vapor permeabilities range from 1.34–6.12 $\times10^{-14}$ kg/(m·s·Pa), while the pre-steady-state values range between 15.71–41.94 $\times10^{-14}$ kg/(m·s·Pa) as shown in Table 1 These results confirm that lasure partially permits water-vapor permeability compared with the uncoated one. Low-density species OPWand SMW showed the highest δ values and the greatest mass change, due to their structure and larger accessible pore volume, compared with other wood species used in both zones (pre-steady and steady zones). In contrast, high-density woods like EUW, BW,

and OW exhibited lower δ values and minimal mass change, conforming the density effect and the wood internal porosity. The water vapor permeability and the mass change showed an inverse relationship with sample density, and a clear dependence on the structural properties of each wood species.

Table 2 Permeability/mass change within lasure coated wood samples

	Density Kg/m^3	δ (steady state) $\times10^{-14}$kg/(m·s·Pa)	δ (pre-steady zone) $\times10^{-14}$ kg/(m·s·Pa)	Mass change at transition point (g)
OPW	301.1	6.12	41.94	14.45
SMW	379.4	6.09	37.00	7.33
GPW	449.3	2.84	27.23	6.30
SW	511.4	1.60	18.37	3.88
OW	682.1	1.38	21.61	3.87
BW	759.9	1.41	15.41	3.32
EUW	952.18	1.34	15.71	3.27

3- Wood coated with commercial adhesive

The permeability behavior of wood coated with commercial adhesives AJ and AX reveals clear density-dependent patterns as shown in Fig.1, 2 for example in case of BW and OW. The steady-state water vapor permeabilities remain relatively low between 0.08–0.36 $\times10^{-14}$ kg/(m·s·Pa) for all species as presented in Table 2.

Similar to other wood species the mass change at the transition point "A", shows a strong inverse relationship with density: lower-density woods e.g., OPW at 301.1 kg/m³ and SMW at 379.4 kg/m³ exhibited noticeably higher mass change 1.34–1.48 g, whereas denser species such as EUW (952.18 kg/m³) recorded the lowest mass changes (0.59–0.64 g).

A moderate negative correlation was observed between wood density and pre-steady-state permeability across all adhesive coated samples, both with the commercial structural adhesive AJ and the custom made AX, with $r = -0.492$, $R^2 = 0.242$, and $p = 0.074$, suggesting that higher-density species tend to exhibit lower initial permeability. Although not statistically significant at the 0.05 level,

the trend indicates that wood density still influences pre-steady vapor diffusion even in the presence of the commercial structural adhesive coatings. The correlation is **moderately negative**, suggesting that higher-density species tend to have lower pre-steady permeability even when coated. R^2 shows that approximately **24% of the variability** in pre-steady permeability is explained by wood density.

These contrasts highlight that permeability behavior cannot be predicted solely from density or wood species type; instead, it emerges from the interaction between wood anatomy, adhesive permeability, and molecular structure of the adhesive. Consequently, each wood species must be evaluated independently and compared with other adhesive or coating materials, to accurately calculate the difference in permeability within the same wood with different conditions (uncoated / coated)

Table 3 Permeability/mass change within wood sample with AJ and AX

	Density Kg/m^3	δ (steady state) $\times10^{-14}$kg/(m·s·Pa)	δ (pre-steady zone)$\times10^{-14}$ kg/(m·s·Pa)	Mass change at transition point (g)
SW_{AJ}	511.4	0.08	4.78	0.37
OW_{AX}	682.1	0.18	3.87	0.59
OW_{AJ}	682.1	0.25	5.38	0.60
EUW_{AX}	952.18	0.21	3.93	0.64
BW_{AX}	759.9	0.29	3.90	0.75
SW_{AX}	511.4	0.24	5.11	0.77
BW_{AJ}	759.9	0.31	5.80	0.93
SMW_{AX}	379.4	0.31	5.86	0.94
SMW_{AJ}	379.4	0.24	11.49	1.05
GPW_{AX}	449.3	0.36	7.53	1.15
EUW_{AJ}	952.18	0.32	10.09	1.20
GPW_{AJ}	449.3	0.32	10.64	1.22
OPW_{AJ}	301.1	2.53	21.45	1.34
OPW_{AX}	301.1	0.56	8.91	1.48

4- Wood with custom-made synthesized polymer

A consistent pattern becomes apparent when comparing the permeability behavior in the pre-steady Fig. 1; Table 3 and steady-state Fig. 2; Table 4 zones for the investigated wood species coated with custom-made synthesized polymers S1–S5. Despite the systematic control of adhesive formulations, the resulting permeability performance varied significantly among the different wood species. This clearly indicates that the intrinsic characteristics of the wood, particularly density, anatomical structure, and porosity play a decisive role in governing overall vapor transport behavior. Therefore, the final permeability of the adhesive–wood system is not determined solely by the adhesive itself, but rather by the interaction between the adhesive properties and the specific structural features of each wood species. In both the pre-steady and steady-state zones, the water vapor permeability consistently reflected the structural characteristics of the wood. Dense and anatomically compact species, such as EUW (952.18 kg/m^3), exhibited the lowest permeability values, whereas highly porous, low-density species, such as OPW (301.1 kg/m^3), consistently showed the highest vapor permeability. Mass change showed an inverse relationship with density: low-density woods accumulated the highest mass change, whereas high-density woods exhibited the lowest mass change even when water vapor permeability were comparable. Within each wood species, water vapor permeability among different MW adhesive systems remained relatively close, yet mass-change values diverged significantly. This again reflects the strong role of density and wood structure properties storage capacity, where lower-density woods consistently absorbed more moisture despite comparable δ values.

Although the steady- and pre-steady diffusion parameters G and δ indicate differences between coated and uncoated samples, their slope-based nature limits their ability to fully reflect the actual blocking efficiency of the adhesive layers. Since permeability is calculated as a mass change per unit time,

a large mass increase over a long period may numerically resemble a small mass increase over a shorter period, leading to comparable rate values despite fundamentally different diffusion behaviors. This effect becomes evident when comparing the steady-to-pre-steady ratios of the uncoated and samples coated with lasure, which appear proportionally similar, although their total accumulated masses differ substantially. For example, at the transition point A, the y_A coordinate of SMW_N reached 11.36 g, whereas SMW_{AJS} reached only 1.05 g and SMW_{AXS} 0.95 g, corresponding to an absolute difference of approximately 10.3–10.4 g. Such a large disparity directly reflects the effective vapor-blocking action of the adhesive layer. In contrast, when evaluating the late-stage slope between 350–400 h (Δm/50 h), the calculated rate values for S1–S5 and AX become relatively close, which does not proportionally represent their markedly different accumulated mass levels. This confirms that slope-derived parameters alone cannot adequately describe the hindering or promoting effect of adhesive systems. Therefore, the y_A coordinate of point A, representing the total mass uptake at the diffusion transition, provides a more physically meaningful and sensitive indicator for assessing adhesive-induced diffusion blocking effect.

Table 4 Permeability/mass change within a wood sample with a custom-made synthesized polymer at pre steady zone

No.	Type	Density Kg/m^3	$\delta \times 10^{-14}$ kg/(m·s·Pa)	Mass change at transition point (g)
1	EUW_{S1}	952.18	5.29	0.73
2	BW_{S1}	759.9	5.43	0.87
3	SW_{S1}	511.4	6.98	0.97
4	SMW_{S1}	379.4	8.31	1.10
5	OW_{S1}	682.1	8.40	1.19
6	BW_{S2}	759.9	9.06	1.44
7	EUW_{S2}	952.18	9.27	1.23
8	OW_{S2}	682.1	11.97	1.68
9	SW_{S2}	511.4	11.98	1.51

10	OPW_{S1}	301.1	12.50	1.73
11	SMW_{S2}	379.4	13.75	1.82
12	BW_{S3}	759.9	14.34	2.21
13	EUW_{S3}	952.18	14.85	1.89
14	GPW_{S1}	449.3	15.22	1.86
15	SW_{S3}	511.4	19.30	2.31
16	OW_{S3}	682.1	19.50	2.89
17	BW_{S4}	759.9	20.30	3.12
18	GPW_{S2}	449.3	20.88	3.29
19	OPW_{S2}	301.1	20.90	2.85
20	EUW_{S4}	952.18	20.98	2.67
21	SMW_{S3}	379.4	22.08	2.79
22	OW_{S4}	682.1	22.75	4.46
23	SW_{S4}	511.4	24.32	3.99
24	BW_{S5}	759.9	31.08	4.66
25	SMW_{S4}	379.4	31.63	3.86
26	EUW_{S5}	952.18	32.41	3.99
27	OPW_{S3}	301.1	33.75	4.29
28	GPW_{S3}	449.3	34.60	4.93
29	OW_{S5}	682.1	40.42	5.61
30	SW_{S5}	511.4	43.15	4.73
31	GPW_{S4}	449.3	44.47	6.15
32	GPW_{S5}	449.3	46.63	7.90
33	OPW_{S4}	301.1	47.76	6.03
34	SMW_{S5}	379.4	49.98	5.59
35	OPW_{S5}	301.1	73.31	9.14

Table 5 Permeability/mass change within a wood sample with a custom-made synthesized polymer at a steady state zone

No.	Type	Density Kg/m^3	δ $\times 10^{-14}$ kg/(m·s·Pa)	Mass change at transition point (g)
1	EUW_{S1}	952.18	0.21	0.73
2	BW_{S1}	759.9	0.28	0.87
3	BW_{AJ}	759.9	0.31	0.94
4	SW_{S1}	511.4	0.28	0.97
5	OW_{S1}	682.1	0.35	1.19
6	EUW_{S2}	952.18	0.35	1.23
7	BW_{S2}	759.9	0.46	1.44
8	SW_{S2}	511.4	0.41	1.51
9	OW_{S2}	682.1	0.49	1.68

10	OPW_{S1}	301.1	0.55	1.73
11	SMW_{S2}	379.4	0.51	1.82
12	GPW_{S1}	449.3	0.50	1.86
13	EUW_{S3}	952.18	0.52	1.89
14	BW_{S3}	759.9	0.70	2.21
15	SW_{S3}	511.4	0.61	2.31
16	EUW_{S4}	952.18	0.74	2.67
17	SMW_{S3S}	379.4	0.77	2.79
18	OPW_{S2}	301.1	0.93	2.85
19	OW_{S3}	682.1	0.88	2.89
20	BW_{S4}	759.9	0.98	3.12
21	GPW_{S2}	449.3	1.06	3.29
22	SMW_{S4}	379.4	1.04	3.86
23	EUW_{S5}	952.18	1.08	3.99
24	SW_{S4}	511.4	1.32	3.99
25	OPW_{S3}	301.1	2.03	4.29
26	OW_{S4}	682.1	1.73	4.46
27	BW_{S5}	759.9	1.44	4.66
28	SW_{S5}	511.4	1.20	4.73
29	GPW_{S3}	449.3	1.47	4.93
30	SMW_{S5}	379.4	1.43	5.59
31	OW_{S5}	682.1	1.64	5.61
32	OPW_{S4}	301.1	4.66	6.03
33	GPW_{S4}	449.3	1.79	6.15
34	GPW_{S5}	449.3	2.69	7.90
35	OPW_{S5}	301.1	9.80	9.14

Overall conclusion: Based on diffusion tests conducted on uncoated, lasure-coated, and high MW, custom made polyol-coated samples from seven wood species, it was concluded that wood density strongly influences pre-steady-state diffusion, but has little effect on steady-state permeability. Consequently, correlations between density and permeability indicate that the pre-steady zone is the most suitable region for evaluating water vapor diffusion behaviour of adhesives—particularly their barrier or blocking effect—while the steady-state portion of the mass change curve is less informative in this regard.

Conclusion and theses

1- Based on the results, it can be concluded that commercial structural adhesives impede water-vapor diffusion through the adhesive layer in bonded wood, creating a vapor-blocking effect that induces internal strains. Diffusion is hindered approximately five times more compared to lasures.

2- Based on diffusion tests conducted on uncoated, lasure-coated, and high MW, custom made polyol-coated samples from seven wood species, it was concluded that wood density strongly influences pre-steady-state diffusion, but has little effect on steady-state permeability. Consequently, correlations between density and permeability indicate that the pre-steady zone is the most suitable region for evaluating water vapor diffusion behaviour of adhesives—particularly their barrier or blocking effect—while the steady-state portion of the mass change curve is less informative in this regard

3- Based on the results the following exponential relation is valid between the density and the permeability is the steady state zone:

$$\delta_{\text{steady}}(\rho) \approx 12.31\, e^{-0.00233\,\rho} \text{x } 10^{-14}$$

and in the pre-steady state zone:

$$\delta_{\text{pre-steady}}(\rho) \approx 65.95\, e^{-0.00151\,\rho} \text{x } 10^{-14}$$

4- Based on the results it was proved that the MW of the adhesive is responsible for blocking or supporting the water vapor diffusion. Low-MW adhesive systems (MW≈2000) restrict diffusion due to their compact polymer structure, whereas high-MW formulations (MW 5000–6000) exhibit wider molecular spacing, allowing greater penetration of water vapor or even liquid water. Therefore, controlling the adhesive molecular weight represents an effective approach for regulating vapor diffusion and vapor-diffusion-induced strains in bonded wood structures.

5- The water vapor diffusion of all the tested different wood species with different MW adhesives can be described by the following generalized hyperbolic tangential equation:

$$\Delta m = b_1 * \tanh(b_0 * t) \qquad [\boldsymbol{g}] \qquad R^2 \geq 70\%$$

the b_0 and b_1 are empirical parameters of the mass change function and are both wood species and adhesive MW specific.

6- The pre-steady diffusion zone revealed significant differences in water-vapor diffusion behavior among different wood species and adhesive molecular-weight systems. In contrast, evaluating diffusion solely under steady-state conditions, as specified by ISO 12572 and ASTM E96, may obscure the true vapor-blocking performance of adhesive layers. Consequently, identifying the (x, y) coordinates of the A-point (transition point) on the diffusion curve provides a more sensitive and reliable parameter for determining whether an adhesive system hinders or facilitates water-vapor diffusion.

7- while coatings determined the **absolute strain level and temporal profile**, the fundamental trend — that strain decreases with increasing wood density — remained consistent. This highlights that pre-steady-state strain is a sensitive and informative indicator of how wood species respond mechanically to moisture, and that coating type primarily affects the **rate and magnitude** of the response rather than the density-driven trend itself

Publications

1- **Zinad, Omar saber** and Csiha, Csilla (2024) Review on water vapor diffusion through wood adhesive layer. Journal of the Korean Wood Science and Technology, 52 (4). pp. 301-318. ISSN 1017-0715 (**Q2**)
2- Csiha, C., Hofmann, T., & **Zinad, O. S**. (2025). Investigation into Adhesion of Coatings and Adhesives of Eucalyptus and Grey Poplar for Building Applications. Forests, 16(2), 287. (**Q1**)
3- **Zinad, Omar saber** and Csiha, Csilla (2025). Investigation of Adhesion Properties of Red Eucalyptus Structural Wood in Relation to Its Chemical Composition . Book of abstract of 8th International Conference on Process Technologies for the Forest and Biobased Products Industries 2025 Conference: Kuchl, Austria 2025.09.18. - 2025.09.19. (Salzburg University of Applied Sciences Design and Green Engineering Department Campus Kuchl) : Salzburg University of Applied Sciences Design and Green Engineering Department Campus Kuchl, pp 39.
4- **Zinad, Omar saber** and Csiha, Csilla (2025). Water Vapor Transport Challenges Across Structural Wood Adhesive Layer. Book of abstract of 8th International Conference on Process Technologies for the Forest and Biobased Products Industries 2025 Conference: Kuchl, Austria 2025.09.18. - 2025.09.19. (Salzburg University of Applied Sciences Design and Green Engineering Department Campus Kuchl) : Salzburg University of Applied Sciences Design and Green Engineering Department Campus Kuchl, pp 38
5- **Zinad, O. S.,** & Csiha, C. (2024). Improving sustainability of mortar by wood-ash and Nano-SiO2. Case studies in chemical and environmental engineering, 9, 100597.(**Q1, D1**)
6- **Zinad, Omar Saber ,** Csiha Csilla , Al-Attar Alya'a Abas. Cost Analysis of Sustainable Concrete Production Using Waste Nanoparticles In: társadalom – gazdaság – természet: szinergiák a fenntartható fejlődésben (nemzetközi tudományos konferencia a magyar tudomány ünnepe alkalmából):KONFERENCIAKÖTET, Conference: Sopron, Hungary 2022.11.03-2022.11.03. Sopron: University of Sopron Press, pp 585-593 (2023)
7- **Zinad Omar Saber** ,Csiha Csilla, Zinad Dhafer, Fahem Al-Mamoori Ali (2024). Ecological and Health Implications of Microplastics in Water: A Short Review In: Csiha Csilla (Csiha Csilla Faanyagok felületkezelése és ragasztása) SOE/ FWECI/ Institute of Applied Sciences (eds.) Wood 4 Sustainability : Processing, Construction, Products and Design 2024

Sopron: University of Sopron Press, Soproni Egyetem Faipari Mérnöki és Kreatívipari Kar, pp 121-130

8- **Zinad Omar Saber** , Csilla Csiha. Study on Moisture Diffusion in Structural Adhesives. (2025), Sopron: University of Sopron Press, Language: English | ISBN: 9789633345412 1

9- **Zinad, Omar saber** and Csiha, Csilla (2025). Evaluation of water vapor diffusion of Empress tree hybrid samples with adhesive. Book of abstract of 14. International Conference on Wood Science and Engineering in the Third Millennium (ICWSE 2025) Conference: Transilvania" University of Brasov (Romania), Faculty of Furniture Design and Wood Engineering, and it will be held between 6-8 November 2025, at the Aula of the "Transilvania" University of Brasov

Referance

Csiha, C., & Gurau, L. (2011). Study on the influence of surface roughness on the adhesion of water based PVAC. *Proceedings of International Conference "Wood Science and Engineering", Brasov, Romania*, 411–419.

Csiha, C., Hofmann, T., & Zinad, O. S. (2025). Investigation into Adhesion of Coatings and Adhesives of Eucalyptus and Grey Poplar for Building Applications. *Forests*, *16*(2), 1–14. https://doi.org/10.3390/f16020287

De Meijer, M., & Militz, H. (2000). Moisture transport in coated wood. Part 1: Analysis of sorption rates and moisture content profiles in spruce during liquid water uptake. *Holz Als Roh - Und Werkstoff*, *58*(5), 354–362. https://doi.org/10.1007/s001070050445

Dietsch, P., Franke, S., Franke, B., Gamper, A., & Winter, S. (2015). Methods to determine wood moisture content and their applicability in monitoring concepts. *Journal of Civil Structural Health Monitoring*, *5*(2), 115–127. https://doi.org/10.1007/s13349-014-0082-7

Elkhal, M., Hakam, A., Ez-Zahraouy, H., Hader, A., Tanasehte, M., & Ziani, M. (2022). Mechanical and physical properties of the date palm stem (Phoenix dactylifera L.) in Morocco. *European Journal of Wood and Wood Products*, *80*(3), 693–703.

Fick, A. (1855). On liquid diffusion. *The London, Edinburgh, and Dublin Philosophical Magazine and Journal of Science*, *10*(63), 30–39. https://doi.org/10.1080/14786445508641925

Franke, B., Franke, S., Schiere, M., & Müller, A. (2016). Moisture diffusion in wood - Experimental and numerical investigations. *World Conference on Timber Engineering - WCTEAt: Vienna, AustriaVolume*.

Arno Frühwald. (2017). Oil Palm Trunk Utilization. *International Academy of Wood Science*, 20.

Athawale, V. D., & Nimbalkar, R. V. (2010). Emulsifyable air drying urethane alkyds. *Progress in Organic Coatings*, *67*(1), 66–71. https://doi.org/10.1016/j.porgcoat.2009.09.017

Bekhta, P., Ortynska, G., & Sedliacik, J. (2015). Properties of Modified Phenol-Formaldehyde Adhesive for Plywood Panels Manufactured from High Moisture Content Veneer. *Drvna Industrija*, *65*(4), 293–301. https://doi.org/10.5552/drind.2014.1350

Bomba, J., Šedivka, P., Böhm, M., & Devera, M. (2014). Influence of Moisture Content on the Bond Strength and Water Resistance of Bonded Wood Joints. *BioResources*, *9*(3), 5208–5218. https://doi.org/10.15376/biores.9.3.5208-5218

Caudullo, G., Tinner, W., & De Rigo, D. (2016). Picea abies in Europe: distribution, habitat, usage and threats. In *European Atlas of Forest Tree Species*. Publications Office of the European Union, Luxembourg.

Thybring, E. E., Thygesen, L. G., & Burgert, I. (2017). Hydroxyl accessibility in wood cell walls as affected by drying and re-wetting procedures. *Cellulose*, *24*(6), 2375–2384. https://doi.org/10.1007/s10570-017-1278-x

Time, B. (1998). *Hygroscopic moisture transport in wood. Dr ing*. Norwegian University of Science and Technology, Trondheim.

Tsushima S., K. Teranishi, Hirai. S. (2005). Water diffusion measurement in fuel-cell SPE membrane by NMR. *Energy*, *30*(2–4), 235–245.

Ülker, O. (2016). Wood Adhesives and Bonding Theory. In *Adhesives - Applications and Properties* (pp. 271–288). https://doi.org/10.5772/65759

Utsumi, Y., Sano, Y., Fujikawa, S., Funada, R., & Ohtani, J. (1998). Visualization of cavitated vessels in winter and refilled vessels in spring in diffuse-porous trees by cryo-scanning electron microscopy.

Plant Physiology, *117*(4), 1463–1471. https://doi.org/10.1104/pp.117.4.1463